Stem Cell Rev and Rep (2009) 5:410–419
DOI 10.1007/s12015-009-9092-y

PROTOCOLS

A Three Dimensional Anchorage Independent *In Vitro* System for the Prolonged Growth of Embryoid Bodies to Study Cancer Cell Behaviour and Anticancer Agents

Chui-Yee Fong · Li-Ling Chak · Arjunan Subramanian · Jee-Hian Tan · Arijit Biswas · Kalamegam Gauthaman · Mahesh Choolani · Woon-Khiong Chan · Ariff Bongso

Published online: 16 September 2009

Abstract We describe a three dimensional (3D) anchorage independent *in vitro* protocol for the prolonged growth of human embryoid bodies (EBs) up to 90 days. We grew hESCs (46XX) in methylcellulose (MC) in motion culture in the presence of EB medium (EB), EB medium with Matrigel (EB + MAT), bulk culture medium (BCM), and BCM medium with Matrigel (BCM + MAT). All four experimental groups produced embryoid bodies (EBs) which with prolonged growth to 90 days acquired blood vessels and tissues from all three germ layers. Based on histology, microarray gene expression profiles and the definition for experimental teratomas, we could classify the EBs into early EBs, mature EBs and teratomas. The EB + MAT group produced the highest number of teratomas and their microarray data suggested the presence of inductive microenvironment niches and activation of pathways for self-organization, morphogenesis and growth. When we microinjected hepatocarcinoma-Green Fluorescent Protein cells (HepG2-GFP) (46XY) into the teratomas, after 10 days the HepG2-GFP cells had grown inside the teratoma as confirmed by confocal microscopy and SRY gene analysis. This 3D-MC-(EB + MAT) *in vitro* system requires few cells to produce many teratomas, can be used to test pluripotency of potential human embryonic and induced pluripotent stem cell lines (hESC, hiPSC), and is an experimental humanized platform to study cancer cell behavior.

Keywords Embryoid bodies · Histology · Human embryonic stem cells · *In vitro* teratoma assay · Microarray · Microinjection

C.-Y. Fong · A. Subramanian · A. Biswas · K. Gauthaman · M. Choolani · A. Bongso (✉)
Department of Obstetrics & Gynecology,
Yong Loo Lin School of Medicine, National University of Singapore,
Kent Ridge, Singapore 119074
e-mail: obgbongs@nus.edu.sg
URL: www.nus.edu.sg

L.-L. Chak · J.-H. Tan · W.-K. Chan
Department of Biological Sciences,
National University of Singapore,
Kent Ridge, Singapore 119074

Introduction

Human embryonic and induced pluripotent stem cells (hESCs, hiPSCs) are pluripotent sources of stem cells derived from preimplantation embryos and reprogrammed somatic cells respectively. Their ability to differentiate into tissues from all three primordial germ layers allows the generation of a wide spectrum of tissues for the potential treatment of many diseases by transplantation therapy. This plasticity was confirmed by the production of experimental teratomas injected at various sites in immunodeficient mice [1–3]. Such experimental teratomas have been defined as structures characterized by the presence of haphazardly arranged differentiated tissues representing the three embryonic germ layers and originating from a pluripotent precursor [4]. This ability to produce a teratoma *in vivo* in an animal model has been claimed as the gold standard [5] for evaluating the pluripotency and quality of hESCs and hiPSCs, and has also been an experimental platform for studying the growth and invasiveness of tumor cells [6, 7].

The production of *in vivo* mouse teratomas has several important issues. Immunodeficient mice are expensive and many have to be sacrificed as part of the experiment. More importantly, the use of these models poses ethical concerns as some interpret these as a form of human-animal chimera [8]. Their use as an experimental platform to study tumor cell invasion adds credence to the proposition that these are

in fact human-animal chimeras. Moreover blood vessels from the host animal environment invade the human teratoma making evaluations unreliable [9]. The development of *in vitro* teratomas would provide stem cell and cancer scientists with a cheaper and ethically acceptable alternative for research. Potentially such an *in vitro* model would allow a more defined human microenvironment to study cell fate decisions in early human development, toxicity testing, screening of novel therapeutic strategies and cancer behavior specifically involving the facilitation or inhibition of angiogenesis and metastasis. It would also allow us to better understand the pathogenesis of teratoma formation and to help devise strategies for preventing their occurrence for safer cell based therapies.

hESCs and hiPSCs produce embryoid bodies (EBs) on non-adherent tissue culture plates in the presence of simple EB medium (DMEM medium + serum, without supplements). Such two dimensional (2D) *in vitro* systems have their shortcomings in that the EBs can be sustained for only short periods of time and the number and types of lineages within them are inconsistent [10, 11]. Itskovitz-Eldor et al [10] grew hESCs in suspension in the presence of EB medium to generate EBs which were grown for a continuous period of 14 days and analyzed for histology and genomic expression of lineage-specific markers using RT-PCR and *in situ* hybridization. They showed gradual increase in size and transformation of the EBs into cystic structures up to 14 days. They classified their EBs as I (simple), II and III (cavitated) and IV (cystic). Twenty days after initiation, 20–90% of the structures became cystic. Histological sections of their Day 20 EBs (which was the maximum duration they grew the EBs *in vitro*) showed the presence of a single cell layer of endodermal-like cells in the periphery and epithelial cells surrounding a lumen in the center. Later, Karbanova and Mokry [11] examined the histology of EBs arising from the aggregation of murine embryonic stem cells (mESCs) after 7, 12, 18 and 26 days of *in vitro* culture. Solid EBs transformed to cystic EBs with spontaneous differentiation in Day 3 EBs. On histology, Day 7 old EBs had a regular round shape, contained only one cell type with prominent cell death in the centre resulting in a cavity. Eighteen day EBs showed reticular fibres, surface endodermal epithelial cells, some smooth muscle cells and fibronectin-positive fibres lining blood vessels. *In situ* immunotyping showed positive alpha fetoprotein (AFP) endodermal and myogenic cells that were positive for desmin, myogenin and actin. Rust et al [12] showed that EBs derived from hESCs up to 10 days expressed genes characteristic of the visceral endoderm but only a minority expressed markers of the primitive streak and definitive endoderm. Their EBs embedded in a Matrigel matrix however lacked the presumptive visceral endoderm but upregulated expression of gastrulation-related genes. None of the EB studies demonstrated the consistent existence of lineages from all three germ layers (ectoderm, mesoderm and endoderm).

Most normal somatic cells are capable of growing on plastic surfaces in a two dimensional (2D) *in vitro* environment with contact inhibition and anchorage dependence. However, three-dimensional (3D) anchorage independent cell growth is the hallmark of cancer cells and since hESCs behave like cancer cells, we examined the ability of a 3D *in vitro* system (containing methylcellulose and Matrigel in the presence of simple or complex culture media), to mature EBs into teratomas after prolonged growth *in vitro.*

Materials

Cell Culture

1. HES3 (46XX) (ES Cell International, Singapore Ltd)
2. HepG2 (46XY) (American Type Culture Collection, ATCC, Maryland, USA)
3. HepG2-Green Fluorescent Protein (HepG2-GFP) (Gift from Dr Gan Shu Uin, National University of Singapore)
4. Mitomycin-C (National University Hospital Singapore pharmacy)
5. Mouse embryonic fibroblasts (MEF)
6. Bulk culture medium (BCM) [KnockOut DMEM medium (Invitrogen, CA, USA) supplemented with 20% KO serum replacement, 0.1 mM ß mercaptoethanol, 1 mM glutamine, 0.1 nM nonessential amino acids, 50 units /ml penicillin, 50 µg/ml streptomycin, 1:200 dilution of ITS (insulin-transferrin-selenium) (Invitrogen) and 16 ng/ml bFGF (Chemicon, CA, USA)]
7. HepG2 medium [(DMEM medium, 10% FBS (Biochrome, Berlin), 1 mM glutamine, 50 units/ml penicillin and 50 µg/ml streptomycin (Invitrogen)]
8. 25 cm^2 sterile plastic flasks (Becton Dickinson, USA)
9. 1 ml sterile Organ culture dishes (Becton Dickinson, USA)
10. Incubator (5% CO_2 in air)
11. Sterile glass Pasteur pipettes
12. Sterile plastic serological pipettes (Becton Dickinson, USA)

3D Methylcellulose Anchorage Independent Growth System

1. Methylcellulose (MC) (R & D systems, Minnesota)
2. EB medium [DMEM medium supplemented with 20% KO serum replacement, 1 mM glutamine, 0.1 nM nonessential amino acids, 0.1 mM ß mercaptoethanol and antibiotic-antimycotic solution (Invitrogen)]

3. 12-well non-adherent plates (Nunclon, Denmark)
4. Incubator (5% CO_2 in air)
5. Phosphate buffered saline (PBS+) (Invitrogen, CA, USA)
6. Sterile serological pipettes (Becton Dickinson, USA)
7. Sterile cell scraper (Corning, USA)
8. Sterile 14 ml Falcon tubes (Becton Dickinson)
9. Centrifuge (Swing-out rotor)
10. Normal Matrigel (BD Bioscience, MA, USA)
11. Mini-see-saw rocker (Stuart, Fisher Sc, MA, USA)

Morphology and Histology

1. Inverted microscope with phase contrast optics
2. 4% buffered formalin
3. Paraffin wax
4. Microtome
5. Eosin stain
6. Hematoxylin stain

RNA/DNA Microarray Analysis

1. Phosphate buffered saline (PBS)
2. RNeasy® Plus Micro Kit (Qiagen)
3. Nanodrop™ 1000 (Thermo Fisher Scientific)
4. Bioanalyzer 2100 (Agilent Technologies)
5. Illumina® TotalPrep RNA Amplification Kit
6. Illumina Beadstation 500GX.
7. BeadStudio Gene Expression Module v3.4
8. Bioconductor lumi package
9. Genesis bioinformatics package
10. TiGER bioinformatics package
11. GeneVenn bioinformatics package

Microinjection of EBs

1. Inverted microscope
2. Narashige micromanipulator
3. Holding pipettes (Humagen, USA)
4. Microinjection pipettes (Humagen, USA)
5. Laser confocal microscope
6. High resolution DNA fragment automated analyser

Methods

Cell Culture

1. Institutional Review Board (IRB) approval was given for the use of human cell lines [HES3 (46XX), HepG2 (46XY) and HepG2-GFP (46XY)] for this study.
2. HES3 cells were cultured on mitomycin-C treated mouse embryonic fibroblasts (MEFs) in BCM.
3. HepG2 and HepG2-GFP cells were grown on plastic in HepG2 medium.

3D Methylcellulose Anchorage Independent Growth System

1. A 1.86% solution of methylcellulose (MC) was prepared in BCM or EB medium.
2. Two ml of MC in EB medium was added into each of 6 wells of 12-well non-adherent plates and two ml of MC in BCM medium added to each of the remaining 6 wells. The plates were equilibrated at 37°C in a 5% CO_2 in air atmosphere for 30 min.
3. HES3 colonies were washed with PBS+, scored with a 1 ml graduated pipette, then scraped mechanically with a cell scraper and the detached cells transferred to four 14 ml Falcon tubes and centrifuged at 300 × g for 5 min.
4. The cell pellet from each tube was resuspended in (a) EB medium (EB); (b) EB medium+0.05% Matrigel (EB + MAT); (c) BCM medium (BCM); (d) BCM medium+0.05% Matrigel (BCM + MAT).
5. Eight million HES3 cells from each of these 4 arms were distributed into each of the respective 12 MC wells. The plates were incubated for 48 h at 37°C in a 5% CO_2 in air atmosphere.
6. After 48 h, 0.5 ml of the respective medium (without Matrigel) was gently added to each well and the plates incubated for a further 48 h.
7. The upper layers of the MC were then gradually removed without removing the cells and replaced with the respective fresh medium.
8. The plates were now placed on a Mini-see-saw rocker and rocked up and down thereafter inside the incubator 9 times per min.
9. Concurrently, two controls were set up. (1) HES3 cells were grown in a conventional 2D EB protocol without MC [13] and (2) HepG2 cells were grown in our 3D-MC system using HepG2 medium. The control dishes were also incubated and rocked 9 times per min.
10. Five replicates were carried out for the experimental and control arms.

Morphology and Histology of HepG2 Cells and EBs

1. The growth and morphological characteristics of the HepG2 cells and hESC-derived EBs in the 2D and 3D systems were monitored and photographed under inverted phase contrast optics over a period of 90 days (Fig. 1) **(See Note 1).**

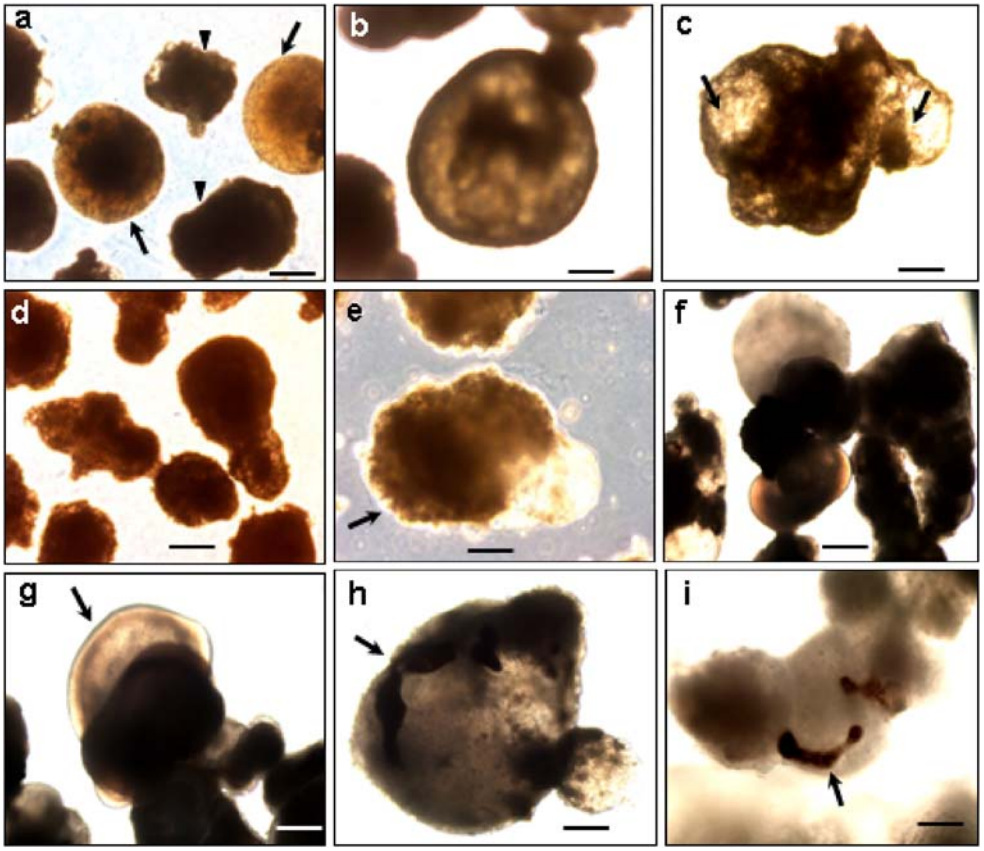

Fig. 1 Inverted phase contrast images of human EBs grown through 90 days in the 3D-MC *in vitro* system. **a** Arrows and arrowheads point at cystic and dense EBs respectively at 7 days. **b** Cystic EB at high magnification. **c** Arrows point at cystic spaces in dense EB at 60 days. **d** Dense EBs at 70 days. **e** Arrow points at peripheral trophoblast-like structures in EB at 60 days. **f–i** Late EBs at 90 days. Note complexity of EBs with arrows pointing at epithelial walls in (**g**), at gut-like structures in (**h**) and at blood vessels in (**i**)

2. Representative EBs at 7, 14, 30, 60 and 90 days were fixed in 4% buffered formalin, then embedded in paraffin and histological sections stained with hematoxylin and eosin. The sections were examined by a qualified histopathologist (Fig. 2) **(See Notes 2 and 3).**

RNA/DNA Microarray Analysis

1. Representative EBs from all 4 experimental arms were collected at 7, 14, 30, 60 and 90 days for microarray analysis.
2. Undifferentiated HES3 (HES3 UD) cells from the same passage on Day 0 were used as controls for microarray analysis.
3. All EBs were rinsed twice with PBS followed by extraction of total RNA using RNeasy® Plus Micro Kit. Total RNA yield was determined using Nanodrop™ 1000 while RNA integrity was evaluated with Bioanalyzer 2100. The Illumina® TotalPrep RNA Amplification Kit was used for the generation of cRNA. First strand cDNA was first prepared from 100 ng of total RNA with the T7 oligo (dT) primer, followed by second strand cDNA synthesis. Amplification of biotinylated cRNA was carried out by *in vitro* transcription with biotin UTP. Following purification, the quantity and integrity of the cRNA was determined using Nanodrop and Agilent Bioanalyzer, respectively. For each Human WG-6 v3.0 Sentrix BeadChip (Illumina) 1.5 µg of biotinylated cRNA was used. The arrays were hybridized and washed according to the protocol, and scanned with the Illumina Beadstation 500GX.
4. Scanned data were retrieved using BeadStudio Gene Expression Module v3.4 and inspected with the quality control parameters. Data was background corrected using the default setting prior to further processing. Probes with measurement value below the background level (detection P value <0.01) were filtered out.
5. Using the Bioconductor lumi package [14], the data was first variance stabilization transformed (VST) [15] and quantile-normalized. The data was mean-centered prior to carrying out two-way hierarchical cluster analysis with Pearson's correlation and average linkage using Genesis [16].
6. Heat maps were generated using the Genesis expression image tool. Gene ontology terms were obtained by DAVID (http://david.abcc.ncifcrf.gov/) [17].
7. Tissue specific gene expression profiles were acquired using TiGER (http://bioinfo.wilmer.jhu.edu/tiger/) [18].

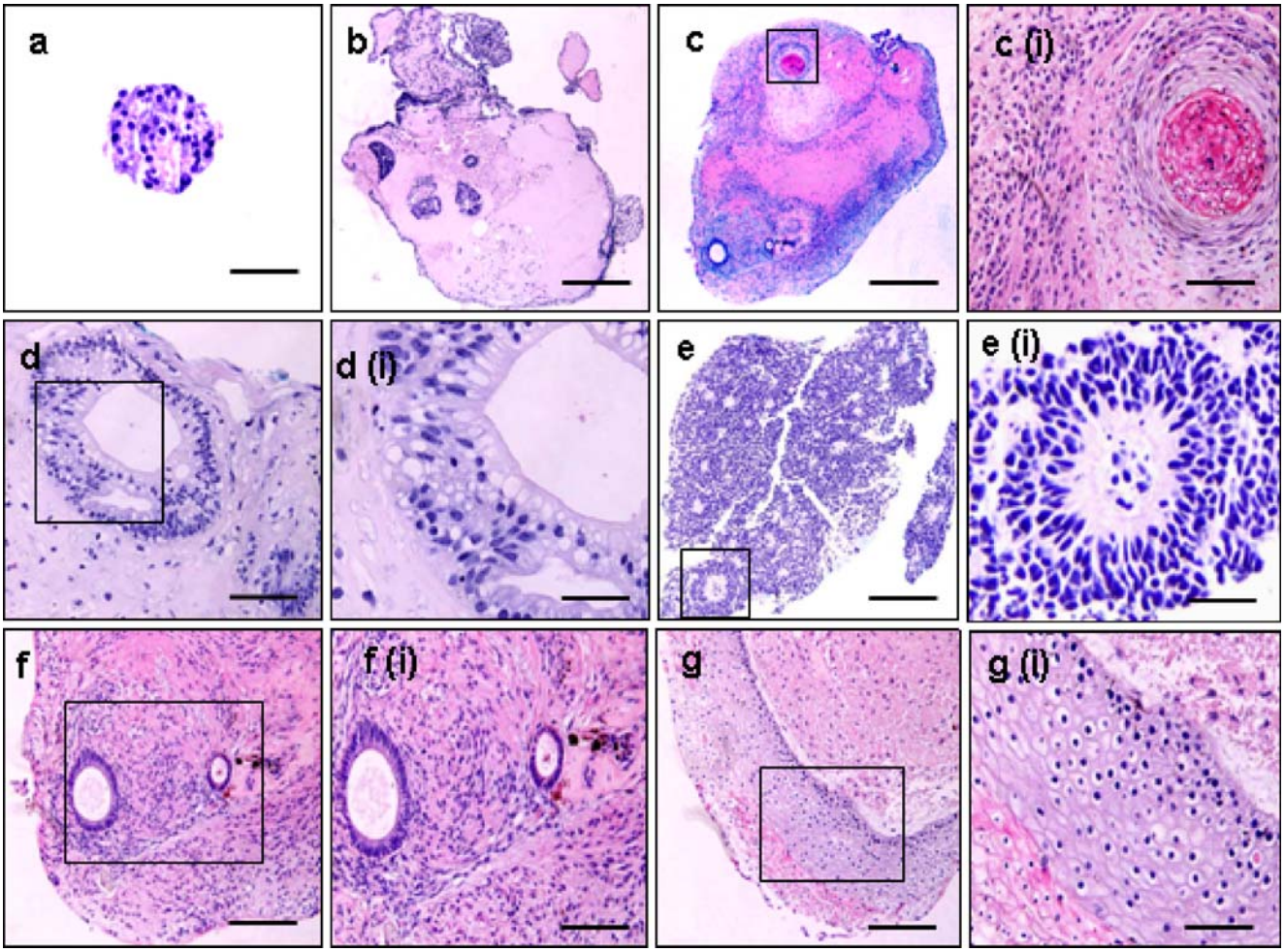

Fig. 2 Histology (H & E) of HepG2 and hESC-derived EBs grown in the 3D MC-Matrigel system. **a** HepG2 cells (controls) growing as healthy circular cell clusters. **[b–g(i)]:** Late EBs (60–90 days) derived from hESCs grown in the same 3D MC-Matrigel. **b**,**c** Complete Late EBs (low magnification) showing many lineages from all three germ layers. **[c(i)]** Keratinized epithelium. **d** Intestinal epithelium. **[d(i)]** Goblet cells in gut. **e** Neural crests (low magnification). **[e(i)]** Neural crest (high magnification). **[f,f(i)]** Low and high magnification of neural tubes and neuroepithelial cells with black pigment. **[g,g(i)]** Low and high magnification of cartilage and bone

8. GeneVenn was used to draw Venn diagrams (http://www.bioinformatics.org/gvenn/) [19].
9. Microarray data were deposited in NCBI GEO (Gene Expression Omnibus) under the accession number GSE16484.
10. For DNA microarray analysis, the most highly expressed genes were selected at a level that was 10 times different compared to undifferentiated hESCs to generate a gene set comprising of 422 genes for analysis.
11. Three distinct clusters, early EBs, mature EBs and teratomas were identified using two-way hierarchical clustering analysis (Fig. 3a). The early EB cluster retained strong expression of key ESC markers but could be clearly demarcated from undifferentiated hESCs by the onset of germ layer lineage markers (Fig. 3b). The mature EB cluster included Day 30 EBs from BCM and BCM + MAT treatments. The presence of bFGF in the BCM appeared to delay the loss of pluripotency markers although the onset of germ layer markers was not largely compromised. Pluripotency markers expression declined sharply in the teratoma cluster (Fig. 3b). More importantly, they showed a strong temporal increase in tissue complexity as indicated by the specific expression of many tissue specific genes (Fig. 3c). The activation of pathways required for self-organization, morphogenesis and growth were also clearly evident (Fig. 3d) (**See Notes 4, 5, 6 and 7).**

Microinjection of EBs

1. Approximately 10–20 HepG2-GFP cells were microinjected using a Narashige micromanipulator into Day 60 old EBs using a holding pipette (inner diameter, 25–30 μm; 35 angle) to hold the EB and a microinjection

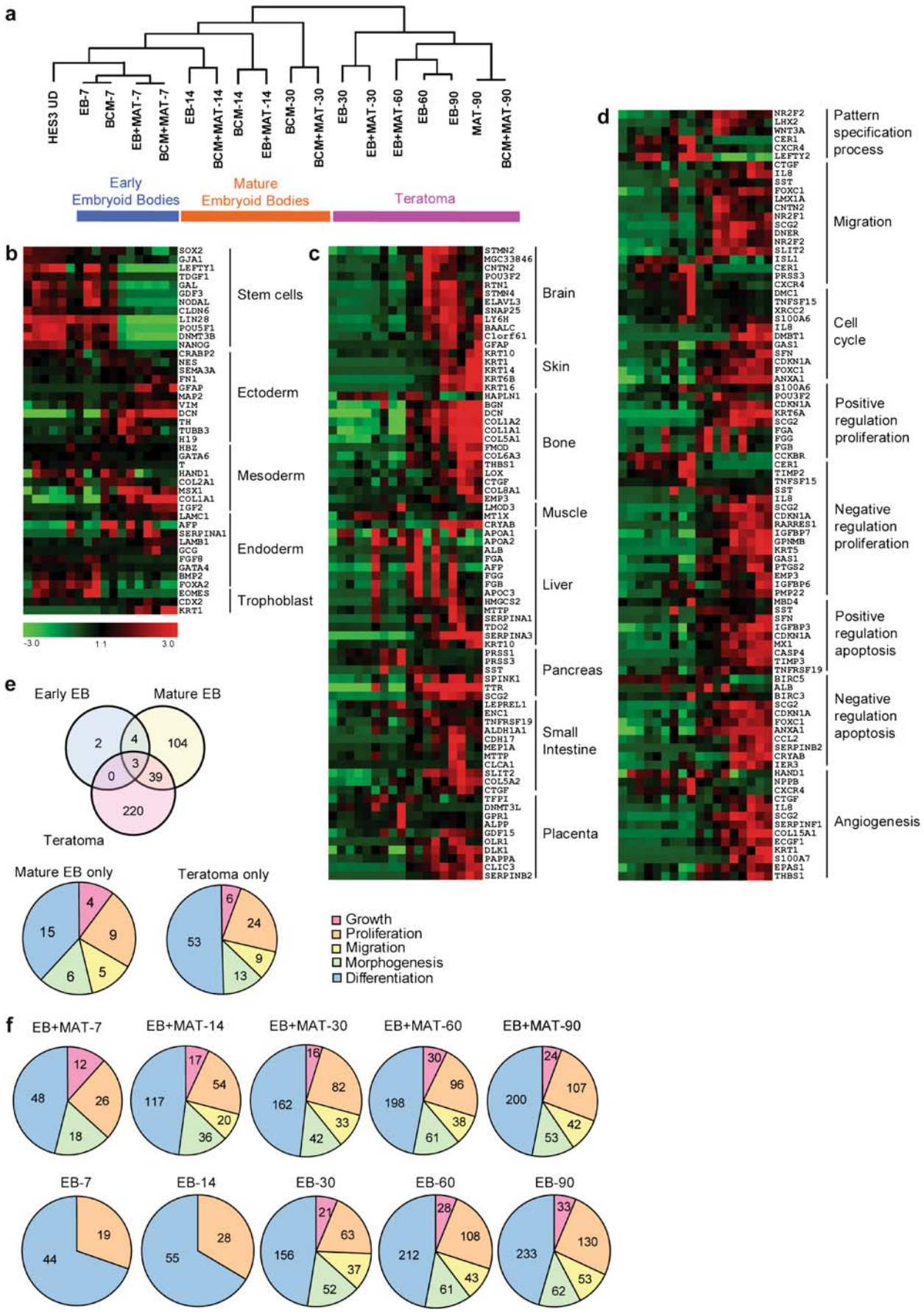
a
HES3 UD
EB-7
BCM-7
EB+MAT-7
BCM+MAT-7
EB-14
BCM+MAT-14
BCM-14
EB+MAT-14
BCM-30
BCM+MAT-30
EB-30
EB+MAT-30
EB+MAT-60
EB-60
EB-90
MAT-90
BCM+MAT-90
Early Embryoid Bodies
Mature Embryoid Bodies
Teratoma
b
Stem cells
Ectoderm
Mesoderm
Endoderm
Trophoblast
c
Brain
Skin
Bone
Muscle
Liver
Pancreas
Small Intestine
Placenta
d
Pattern specification process
Migration
Cell cycle
Positive regulation proliferation
Negative regulation proliferation
Positive regulation apoptosis
Negative regulation apoptosis
Angiogenesis
e
Early EB
Mature EB
Teratoma
Mature EB only
Teratoma only
Growth
Proliferation
Migration
Morphogenesis
Differentiation
f
EB+MAT-7
EB+MAT-14
EB+MAT-30
EB+MAT-60
EB+MAT-90
EB-7
EB-14
EB-30
EB-60
EB-90

◀ **Fig. 3** DNA microarray analysis establishes tissue and developmental complexity of teratomas generated from hESCs *in vitro*. **a** Hierarchical clustering of HES3-derived EBs and teratomas recovers three distinct clusters; early EBs, mature EBs and teratomas. They can be distinguished by substantive temporal increases in developmental complexity as revealed by their gene expression profiles. **b** Genes associated with pluripotent hESCs decreased markedly while lineage markers for germ layers are specifically increased in EBs and teratomas. **c** Genes associated with differentiation into various tissues, as classified by TiGER, showed increasing expression and complexity as development progressed. **d** Biological processes, as identified by Gene Ontology terms, were retrieved using DAVID. The expression of specific genes are strongly demarcated amongst the EBs and teratoma. There was also no aberrant expression of key processes required for tumor formation. **e** Venn diagram illustrates that the majority of the up-regulated genes were expressed predominantly in teratomas or mature EBs. Genes involved in biological processes associated with differentiation and proliferation were particularly prominent in teratomas. The selection criteria for the gene set used for (**b**) to (**e**) were based on an expression level that is 10 times higher or lower compared to HES3 UD. For the heatmaps, the samples are presented as in (**a**). **f** The inclusion of Matrigel during the establishment of EBs resulted in early onset of differentiation as indicated by the comparison between EB and EB + MAT series. Genes associated with growth, migration, and morphogenesis are already prominently up-regulated by Day 7 in EB + MAT

pipette (inner diameter 19–21 μm; 35 angle) to inject the HepG2-GFP cells.

2. The EBs were then washed and cultured in EB medium for 10–20 days without rocking and then subjected to laser confocal microscopy and DNA fragment analysis using real time PCR for the SRY, Y-linked amelogenin and Y-linked PAR2 genes to confirm the growth and presence of the male HepG2-GFP cells within each EB that was derived from female hESCs.
3. By micromanipulation we were able to successfully microinject HepG2-GFP cells into Day 60 EBs grown in the 3D-MC system (Fig. 4a–c).
4. After 10 days, the EBs had grown in size, showed a large area of HepG2-GFP fluorescence on laser confocal microscopy and had a tumor growing within the teratoma on histology (Fig. 4d–f).
5. DNA fragment analysis with real time PCR confirmed the presence of the SRY and Y-linked amelogenin and PAR2 genes from Y chromosomes in the male HepG2-GFP cells within the 46XX hESC-derived teratomas (Fig. 4g) **(See Notes 8, 9 and 10).**

Notes

1. Healthy embryoid bodies (EBs) were generated in all 4 experimental arms and they survived up to 90 days in the 3D-MC system. The EBs in all 4 experimental arms were of two types, dense and cystic. With prolonged culture, they grew in size, became denser, slightly oblong in shape, showed blood vessels and various tissues within them, and became macroscopic from 60 days onwards (Fig. 1). The EBs in the 2D control arm were also of dense and cystic types that grew in size up to 30 days and then started to degenerate. The control HepG2 cells grew as small circular masses in the 3D-MC system similar to anchorage independent growth for cancer cells and did not form EBs. Many more EBs were observed in the 3D-MC system compared to the conventional 2D system. A 60 mm dish containing approximately 8 million HES3 cells produced a mean of 35±3 teratomas in 90 days in the 3D system compared to a mean of 25±4 EBs at 30 days from the same number of HES3 cells in the 2D system. The EB + MAT arm produced the highest percentage (>90%) of teratomas which consistently showed tissues from all three germ layers. The Day 90 teratomas were 6.0–7.0 mm in size for the EB + MAT arm and 2.5–3.5 mm for the other 3D arms, while the Day 30 EBs in the 2D arm were 1.0–1.5 mm. Fewer EBs were generated from the BCM and BCM + MAT arms.
2. On histology, the HepG2 cells showed healthy colonies of equal-sized cells with no evidence of any differentiation (Fig. 2a). The ≤30 day-old healthy EBs grown in the conventional 2D system showed lineages from some germ layers but none showed lineages from all three germ layers. The EBs from the 4 experimental arms contained tissues of various types. We classified these EBs into early EBs, mature EBs and teratomas based on the histology, microarray gene expression profiles and definition for experimental teratomas by Blum and Benvenisty [4]. The early EBs had fewer lineages than the mature EBs while the teratomas consistently contained lineages from all three germ layers. In the *in vitro* teratomas we observed neural rosettes, pigmented neural epithelium, cartilage, columnar epithelium, goblet cells, cystic areas, bone and muscle similar to tissues seen in mature *in vivo* teratomas [Fig. 2b–g(i)]
3. The results of this study showed clearly that the EB + MAT arm was the most superior in terms of teratoma production. There appeared to be progressive increases in differentiation with time in the 3D system and a combination of the methylcellulose, Matrigel and EB medium exposure had the strongest influence on differentiation into teratomas.
4. The histological results showing the presence of heterogeneous cell and tissue types and functional secretory cells in the teratomas were supported by the DNA microarray data and suggested the presence of inductive microenvironment niches. Recently, Wnt signaling in mouse EBs was reported to provide

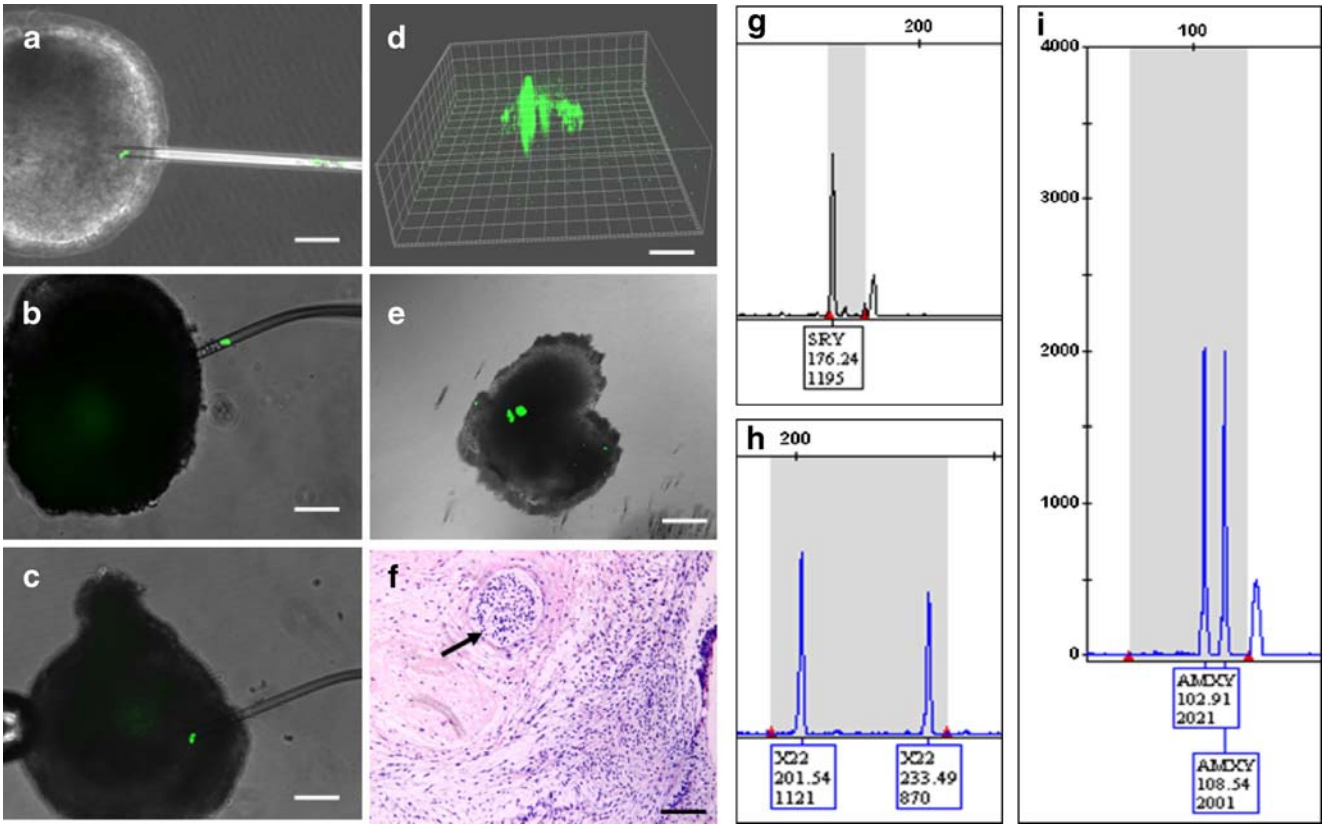

Fig. 4 Microinjection of HepG2-GFP cells into late EBs generated from 3D MC-Matrigel system. **a–c** Green HepG2-GFP cells collected in microinjection pipette and microinjected into 60-day old EB. Note green fluorescent HepG2 cells being deposited from microinjection pipette into EB. **d–e** Ten days later the HepG2 cells grew inside the EB as seen by laser confocal microscopy. **f** Histology section (H & E) of EB showing circular area of HepG2 cells (arrow) growing within late EB. **g** DNA fragment analysis of 3D MC EBs 10 days after microinjection of male HepG2-GFP cells showing SRY, amelogenin (AMXY) and PAR2 (YqPAR2) genes of the Y chromosome

positional cues to establish polarity and guide germ layer progenitor formation [20]. Reorganization to form tissues requires the concerted effort of patterning, cell migration, remodeling via apoptosis and cell growth. Furthermore, the maintenance of any large biological structure necessitates angiogenesis to provide nutrients to the inner compartments. Unlike teratomas established *in vivo*, which are supplied with blood vessels generally formed by the host [2], the 3D-MC *in vitro* system in this study was able to encourage angiogenesis within the EBs (Fig. 3d) and blood vessel formation was obvious. This potentially provides a useful model to study early development without any interference from host interactions.

5. BIRC5 (SURVIVIN) was shown recently to be highly expressed in hESCs and teratomas, but not in mature EBs [21]. These workers concluded that the continued expression of BIRC5 contributes to teratoma formation by hESCs. This is consistent with our microarray data where BIRC5 expression decreased notably from the mature EBs (Fig. 3d). The increased expression of several anti-apoptotic genes viz., CDKN1A [22], SERPINB2 [23] and IER3 [24] suggests that these genes might perform similar functions as BIRC5. Interestingly, many of the up-regulated genes were expressed specifically and predominantly in the *in vitro* teratomas (Fig. 3e). Taken together, the histological and microarray data and the evidence for activation of pathways required for self-organization, morphogenesis and growth firmly suggest that teratomas generated with our 3D-MC system are similar to teratomas established *in vivo* using immunosuppressed mouse hosts.
6. Our histological sections (Fig. 2) did not show any embryonal carcinoma foci that are indicative of teratocarcinoma formation. This is fully supported by the DNA microarray data which did not detect any aberrant expression in the biological processes that are involved in various aspects of cellular regulation (Fig. 3d). Taken together with the lack of stem cell markers, which have been proposed to be associated with malignant cancers [25], the results indicate that these are teratomas and not teratocarcinomas.

7. Matrigel accelerated the process of differentiation as revealed by a marked increase in the number of genes associated with differentiation for Day 7 and Day 14, with the effects wearing off by Day 30 (Fig. 3f). The co-injection of Matrigel with hESCs into mice has been known to increase the frequency of teratoma formation and tissue diversity [2]. This was suggested to occur due to increased graft survival by induced contact inhibition of apoptosis and angiogenesis [26]. Furthermore, our histological data showed that more tissue types were obtained from EB + MAT teratomas (Fig. 2) which agrees with the reported enhancement of EB differentiation with Matrigel [27].
8. The fact that we were able to microinject known quantities of male cancer cells into the female teratomas and confirm their growth, integration and presence within the teratoma illustrates that these *in vitro* teratomas constitute a good humanized microenvironment for studies on cancer behavior and evaluation of anticancer agents before application on human beings. They are also without murine host influences carried by the animal's own blood vessels in hESC-derived SCID mouse in vivo teratomas.
9. This is the first report of a stable *in vitro* system for the growth of teratomas containing lineages from all three germ layers. At least 10 million hESCs are required to induce a single teratoma in SCID mice at 8–12 weeks [28]. In the present study fewer hESCs were required to produce many more teratomas than *in vivo* situations highlighting the efficiency of the 3D system. The methylcellulose and Matrigel probably act like an extracellular matrix (ECM) or scaffold creating cell-matrix interactions that are biologically favorable for cell to cell attachment, migration, proliferation and differentiation [12, 29].
10. Aleckovic and Simon [9] postulated that *in vitro* EBs resemble early post-implantation embryos that are not exposed to a wide range of signals from a corresponding *in vivo* environment, and a controlled EB environment can produce a very useful system for studying cell differentiation by tight regulation of signals received. Such a controlled environment is achievable in the teratomas produced by the 3D-MC-Matrigel-EB medium system in this study. hESC-derived *in vivo* teratomas are seen by some not as a tumor but rather as a failed progress of normal embryonic development due to the incorrect localization of cells [8]. Based on the histological observations of the teratomas generated in the present study, it was clear that although MC-Matrigel-EB medium favored differentiation from all three germ layers, lineage formation was disorganized. If tissues were organized and correctly localized within the *in vitro* teratomas then they may be interpreted as properly formed human embryos that have grown beyond the 14 day primitive streak stage and would thus face ethical issues in their use as platform technology for assays and research. The *in vitro* teratomas generated in the present study are the closest to a controlled ethically comfortable and affordable humanized microenvironment that could replace hESC-induced teratomas in animals to generate meaningful scientific information. Blum and Benvenisty [4] stressed that 2D *in vitro* differentiation of hESCs fails to reach levels of tissue complexity and that a long-term *in vitro* EB model would be very useful for various studies. In conclusion, we suggest that a three-dimensional anchorage independent protocol for the growth of human teratomas *in vitro* is a good alternative to the *in vivo* mouse assay. It requires fewer cells, produces many teratomas, is affordable and non-controversial, and is an experimental humanized platform without host interference to study cancer cell behavior.

Acknowledgements The authors thank Dr Gan Shu Uin (National University of Singapore) for a gift of the HepG2-GFP cells. This project was supported by funds from the National University of Singapore (R-174-000-089-133) and the National Medical Research Council, Singapore (R-174-000-103-213).

References

1. Shih, C. Forman, S. J. Chu, P. & Slovak, M. (2007). Human embryonic stem cells are prone to generate primitive, undifferentiated tumors in engrafted human fetal tissues in severe combined immunodeficient mice. *Stem Cells & Development, 16*, 893–902.
2. Prokhorova, T. A. Harkness, L. M. Frandsen, U. Ditzel, N. Schrøder, H. D. Burns, J. S. et al. (2009). Teratoma formation by human embryonic stem cells is site-dependent and enhanced by the presence of Matrigel. *Stem Cells and Development, 18*, 47–54.
3. Takahashi, K. Tanabe, K. Ohnuki, M. Narita, M. Ichisaka, T. Tomoda, K. et al. (2007). Induction of pluripotent stem cells from adult human fibroblasts by defined factors. *Cell, 131*, 861–872.
4. Blum, B. & Benvenisty, N. (2008). The tumorigenicity of human embryonic stem cells. *Advanced Cancer Research, 100*, 133–158.
5. Brivanlou, A. H. Gage, F. H. Jaenisch, R. Jessell, T. Melton, D. & Rossant, J. (2003). Setting standards for human embryonic stem cells. *Science, 300*, 913–916.
6. Tzukerman, M. Rosenberg, T. Ravel, Y. Reiter, I. Coleman, R. & Skorecki, K. (2003). An experimental platform for studying growth and invasiveness of tumor cells within teratomas derived from human embryonic stem cells. *Proceedings of the National Academy of Sciences USA, 100*, 13507–13512.
7. Tzukerman, M. Rosenberg, T. Reiter, I. Eliezer, S. B. Denkberg, G. Coleman, R. et al. (2006). The influence of a human embryonic stem cell-derived microenvironment on targeting of human solid tumor xenografts. *Cancer Research, 66*, 3792–3801.
8. Lensch, M. W. Schlaeger, T. M. Zon, L. I. & Daley, G. Q. (2007). Teratoma formation assays with human embryonic stem cells: a rationale for one type of human-animal chimera. *Cell Stem Cell, 1*, 253–258.

9. Aleckovic, M. & Simon, C. (2008). Is teratoma formation in stem cell research a characterization tool or a window to developmental biology? *Reproductive Biomedicine Online, 17*, 270–280.
10. Itskovitz-Eldor, J. Schuldiner, M. Karsenti, D. Eden, A. Yanuka, O. Amit, M. et al. (2000). Differentiation of human embryonic stem cells into embryoid bodies comprising the three embryonic germ layers. *Molecular Medicine, 6*, 88–95.
11. Karbanova, J. & Mokry, J. (2002). Histological and histochemical analysis of embryoid bodies. *Acta Histochemistry, 104*, 361–365.
12. Rust, W. L. Sadasivam, A. & Dunn, N. R. (2006). Three-dimensional extracellular matrix stimulates gastrulation-like events in human embryoid bodies. *Stem Cells and Development, 15*, 889–904.
13. Cameron, C. M. Hu, W. S. & Kaufman, D. S. (2006). Improved development of human embryonic stem cell-derived embryoid bodies by stirred vessel cultivation. *Biotechnology and Bioengineering, 94*, 938–948.
14. Du, P. Kibbe, W. A. & Lin, S. M. (2008). Lumi: a pipeline for processing Illumina microarray. *Bioinformatics, 24*, 1547–1548.
15. Lin, S. M. Du, P. Huber, W. & Kibbe, W. A. (2008). Model-based variance-stabilizing transformation for Illumina microarray data. *Nucleic Acids Research, 36*, e11.
16. Sturn, A. Quackenbush, J. & Trajanoski, Z. (2002). Genesis: cluster analysis of microarray data. *Bioinformatics, 18*, 207–208.
17. Huang, D. W. Sherman, B. T. & Lempicki, R. A. (2009). Systematic and integrative analysis of large gene lists using DAVID bioinformatics resources. *Nature Protocols, 4*, 44–57.
18. Liu, X. Yu, X. Zack, D. J. Zhu, H. & Qian, J. (2008). TiGER: a database for tissue-specific gene expression and regulation. *BMC Bioinformatics, 9*, 271–275.
19. Pirooznia, M. Nagarajan, V. & Deng, Y. (2007). GeneVenn: a web application for comparing gene lists using Venn diagrams. *Bioinformation, 1*, 420–422.
20. ten Berge, D. Koole, W. Fuerer, C. Fish, M. Eroglu, E. & Nusse, R. (2008). Wnt signaling mediates self-organization and axis formation in embryoid bodies. *Cell Stem Cell, 3*, 508–518.
21. Blum, B. Bar-Nur, O. Golan-Lev, T. & Benvenisty, N. (2009). The anti-apoptotic gene survivin contributes to teratoma formation by human embryonic stem cells. *Nature Biotechology, 27*, 281–287.
22. Garner, E. & Raj, K. (2008). Protective mechanisms of p53–p21-pRb proteins against DNA damage-induced cell death. *Cell Cycle, 7*, 277–282.
23. Croucher, D. R. Saunders, D. N. Lobov, S. & Ranson, M. (2008). Revisiting the biological roles of PAI2 (SERPINB2) in cancer. *Nature Review Cancer, 8*, 535–545.
24. Wu, M. X. (2003). Roles of the stress-induced gene IEX-1 in regulation of cell death and oncogenesis. *Apoptosis, 8*, 11–18.
25. Ben-Porath, I. Thomson, M. W. Carey, V. J. Ge, R. Bell, G. W. & Regev, A. (2008). An embryonic stem cell-like gene expression signature in poorly differentiated aggressive human tumors. *Nature Genetics, 40*, 499–507.
26. Kleinman, H. K. & Martin, G. R. (2005). Matrigel: basement membrane matrix with biological activity. *Seminars in Cancer Biology, 15*, 378–386.
27. Philip, D. Chen, S. S. Fitzgerald, W. Orenstein, J. Margolis, L. & Kleinman, H. (2005). Complex extracellular matrices promote tissue-specific stem cell differentiation. *Stem Cells, 23*, 288–296.
28. Reubinoff, B. E. Pera, M. F. Fong, C. Y. Trounson, A. & Bongso, A. (2000). Embryonic stem cell lines from human blastocysts: somatic differentiation in vivo. *Nature Biotechology, 18*, 399–404.
29. Mauck, R. L. Li, W. J. & Tuan, R. S. (2009). Microenvironmental determinants of stem cell fate. In U. Meyer, J. Handschel, H. P. Weismann & T. Meyer (Eds.), *Fundamentals of tissue engineering and regenerative medicine*. Berlin: Springer.